

## Article

# Iron and Manganese Oxidation States, Bonding Environments, and Mobility in the Mining-Impacted Sediments of Coeur d'Alene Lake, Idaho: Core Experiments

Gaige Swanson <sup>1</sup>, Jeff B. Langman <sup>2,\*</sup> , Andrew W. Child <sup>3</sup> , Frank M. Wilhelm <sup>4</sup>  and James G. Moberly <sup>3</sup> <sup>1</sup> Department of Water Resources, University of Idaho, Moscow, ID 83844, USA<sup>2</sup> Department of Earth and Spatial Sciences, University of Idaho, Moscow, ID 83844, USA<sup>3</sup> Department of Chemical and Biological Engineering, University of Idaho, Moscow, ID 83844, USA<sup>4</sup> Department of Fish and Wildlife Sciences, University of Idaho, Moscow, ID 83844, USA

\* Correspondence: jlangman@uidaho.edu; Tel.: +1-208-885-0310

**Abstract:** The mobility of a metal in mining-impacted sediments is determined by the environmental conditions that influence the metal's oxidation state and bonding environment. Coeur d'Alene Lake, USA, has been impacted by legacy mining practices that allowed the hydrologic transport of mining waste to the lakebed, resulting in substantial amounts of redox-sensitive Fe and Mn along with Ag, As, Cd, Cu, Hg, Pb, Sb, and Zn. Future lake conditions may include algal blooms and additional algal detritus at the sediment–water interface, which may alter Fe and Mn forms that can influence their, and other metal(loid)s, mobility during seasonal anoxia. Cores of the lakebed sediments were exposed to anoxic and anoxic + algal detritus conditions for 8 weeks. Sediment samples were collected biweekly for analysis of Fe and Mn oxidation states and bonding environments by synchrotron-based X-ray absorption spectroscopy. Over the 8-week period and at a location 12.5 cm deep in the sediments, anoxic and anoxic + algae conditions produced limited changes in Fe and Mn oxidation states and bonding environments. At a location 2.5 cm below the sediment–water interface, the anoxic condition promoted a relatively stable environment in which Fe and Mn oxidation states and bonding environments did not vary greatly during the experiment. At the 2.5 cm depth, the anoxic + algae condition substantially altered the Mn oxidation state distribution and bonding environment, but this condition did not strongly influence the Fe oxidation state distribution or bonding environment. The anoxic + algae condition increased the presence of Mn<sup>3+</sup>, produced Mn<sup>4+</sup> at select times, altered the Mn bonding environment, and temporarily increased the release of Mn into porewater. The algae influence on sediment and porewater Mn likely occurred because of the increased formation of organo-Mn complexes produced during algae-enhanced enzymatic processes. The lack of influence of algal detritus on sediment and porewater Fe and the formation of soluble organo-Mn complexes may limit the potential increase in the mobility of other metal(loid)s with future lake conditions.

**Keywords:** mining-impacted lake; anoxic sediment; algal detritus; iron and manganese oxidation and bonding environment; organo-manganese complexes; Coeur d'Alene Lake



**Citation:** Swanson, G.; Langman, J.B.; Child, A.W.; Wilhelm, F.M.; Moberly, J.G. Iron and Manganese Oxidation States, Bonding Environments, and Mobility in the Mining-Impacted Sediments of Coeur d'Alene Lake, Idaho: Core Experiments. *Hydrology* **2023**, *10*, 23. <https://doi.org/10.3390/hydrology10010023>

Academic Editor: Aronne Armanini

Received: 29 November 2022

Revised: 2 January 2023

Accepted: 9 January 2023

Published: 16 January 2023



**Copyright:** © 2023 by the authors. Licensee MDPI, Basel, Switzerland. This article is an open access article distributed under the terms and conditions of the Creative Commons Attribution (CC BY) license (<https://creativecommons.org/licenses/by/4.0/>).

## 1. Introduction

The impact of legacy mine waste is a global issue that has resulted in extensive metal(loid) contamination of natural environments, such as the substantial contamination of Coeur d'Alene Lake [1–3] in northern Idaho, USA (Figure 1). Remobilization of sediment-bound metals may occur through physical (e.g., current flow) and biochemical (e.g., reduction–oxidation (redox)) processes, particularly during strong seasonal changes in environmental conditions [4–8]. In lacustrine sediments, biochemical processes can be the primary remobilization pathway given limited sediment resuspension [9–11]. In such instances, the seasonal alteration of the lacustrine environment, such as changes in temperature, redox, organic carbon, and microbial populations, can induce or restrict metal

mobility in lakebed sediments [12–18]. An additional influence on metal mobility in such environments is the alteration of redox-sensitive metals, such as iron [Fe] and manganese [Mn] [19]. Changes in Fe and Mn oxidation states and bonding environments can provide sorbing surfaces that allow for the retention of other metal(loid)s and/or produce soluble species/particles that allow transport across the sediment–water interface (SWI) [18,20].

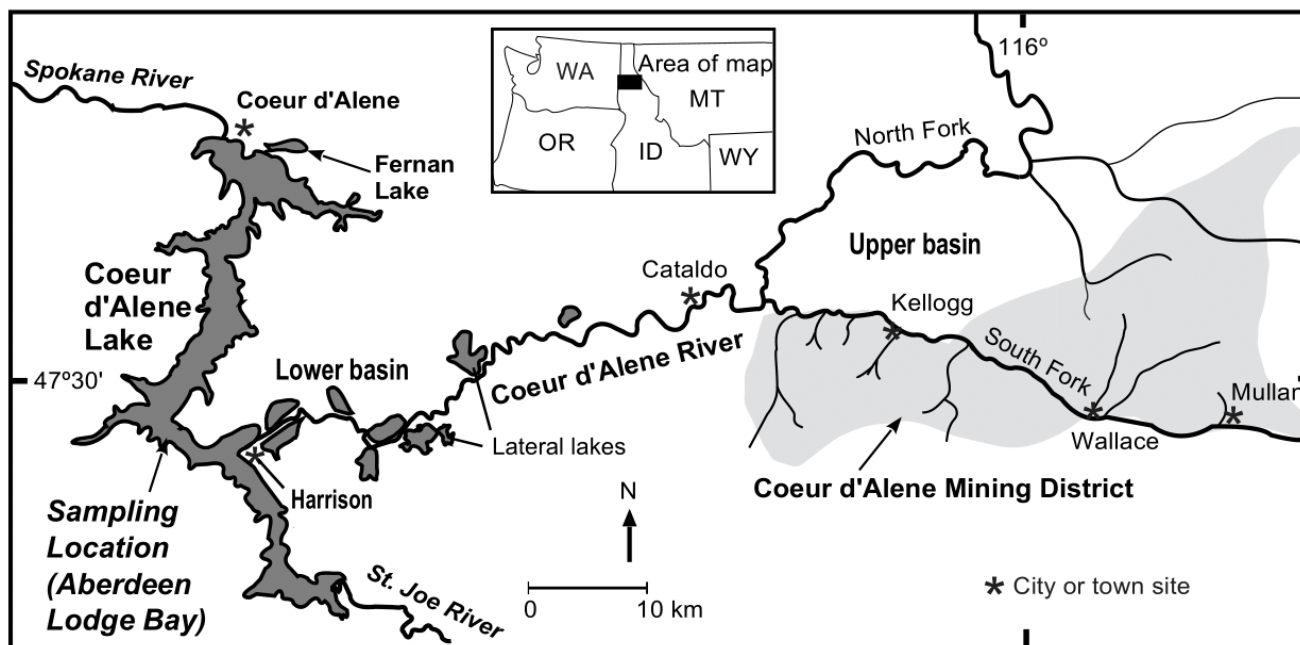


**Figure 1.** Coeur d’Alene Lake, River, and Mining District (Silver Valley) in northern Idaho, USA (modified from [21]).

### 1.1. Legacy Mine Waste Issues, Lakebed Deposition, and Element Mobility

Legacy mining practices in the lead-zinc-silver Coeur d’Alene Mining District (Figure 1) led to the hydrologic transport of tailings and waste rock in the Coeur d’Alene River that resulted in the deposition of 75 Mt of metal(loid)-rich sediments in Coeur d’Alene Lake over the past 100+ years [2,22–24]. The discharge of contaminated sediments to the lake continues to occur and has produced a substantial distribution of the mining-related elements, such as Pb and Zn, in the sediment profile (Figure 2). The basin undergoes strong seasonal physicochemical changes in a snow-dominated, northern climate (dry-summer continental climate (Köppen Dsb)) where remediation efforts have struggled to limit metal loading to the surface water environment [3,25]. This warm, monomictic lake (129 km<sup>2</sup> lake at full summer pool elevation) is seasonally stratified from approximately June to October at a depth of 5 to 8 m, which varies with overall depth, wind exposure, river inflows, and internal waves [26]. During stratification, formation of hypoxic and anoxic water in the hypolimnion [27–29] alters redox conditions at the SWI [30,31], which can remobilize metal(loid)s, such as the 470,000 t of lead [Pb] and substantial masses of silver [Ag], arsenic [As], cadmium [Cd], copper [Cu], Fe, mercury [Hg], Mn, antimony [Sb], and zinc [Zn] present in lake sediments [21,32–36].

Although substantial mine waste remediation has occurred in the Coeur d’Alene River Basin, contaminated sediments continue to be transported to Coeur d’Alene Lake [37]. The continued river input and remobilization of Zn in Coeur d’Alene Lake likely has suppressed algal growth [37–40]. Historically, seasonal conditions at the lake’s SWI have resulted in limited remobilization of sediment-bound metals [1,2,23,30,41–43], yet there is a growing concern of increased metal mobilization because of an expected decrease in Zn inputs from upstream remediation and increases in phosphorus loading [32,44–47]. With a decrease in Zn, future lake conditions may produce algal blooms similar to eutrophic and

mesotrophic lakes in the region [48], which likely will increase the deposition of additional organic matter to the lakebed [49].

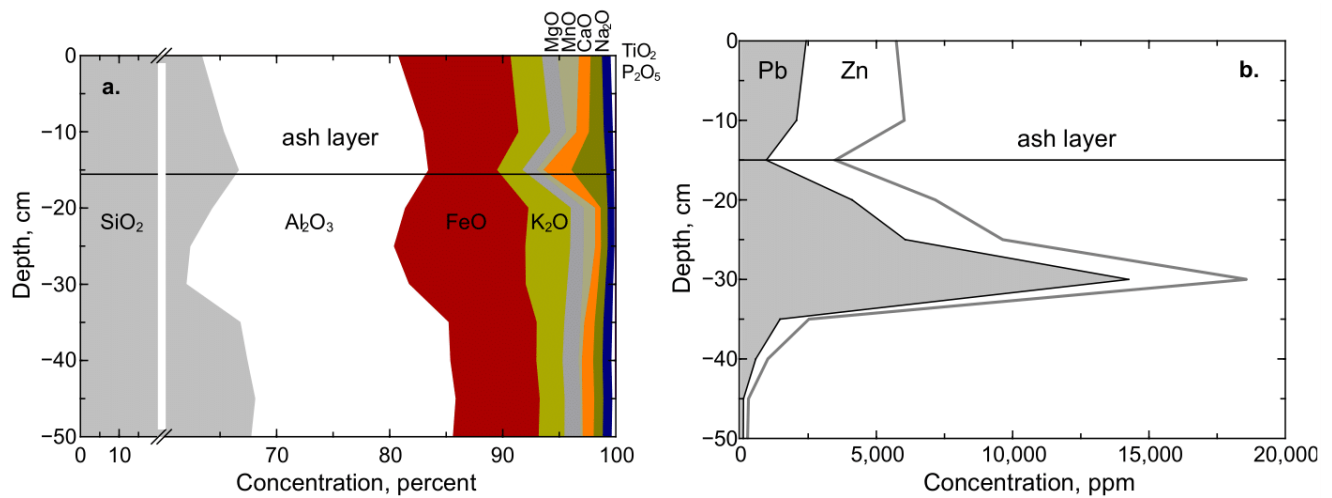


**Figure 2.** Cumulative area graphs of major (a) and trace element (b) concentrations for sediments collected from Aberdeen Lodge Bay in Coeur d’Alene Lake (modified from [21]). Major elements are normalized to 100 percent. Trace element concentrations are not normalized. Ash layer is from the Mount St. Helen’s eruption (1980).

Redox-sensitive elements, such as Fe and Mn, have been identified as controls on the mobility of mining-related metals in Coeur d’Alene Lake sediments [13,29,50]. The presence of Fe and Mn in the mined ore body and resulting waste rock has resulted in the substantial presence of these redox-sensitive elements in lakebed sediments (Figure 2), such as the approximate 10 wt.% as FeO and 1–2 wt.% as MnO in the upper 10 cm [21]. Seasonal variations in the lake environment (e.g., temperature, redox) induce the cycling of Fe and Mn between soluble and insoluble phases [1,13,21,33,39,51]. Harrington et al. [1] hypothesized retention of Fe and Mn in the lake sediments under reducing conditions because of metal-sulfide formation and binding of the metals with organic matter, yet Harrington et al. [1] also described the remobilization of As, Fe, and Mn and their movement upward towards the SWI under oxidizing conditions. This investigation is part of a larger study examining possible changes in the retention/release (mobility) of metal(loid)s found in Coeur d’Alene Lake sediments under the potential future condition of additional algal detritus deposited on the lakebed.

### 1.2. Lake Environment, Sulfur Cycling, and Iron and Manganese Mobility

As part of the larger study that includes this investigation, Langman et al. [21] evaluated changes in sulfur [S] oxidation states and bonding environments in Coeur d’Alene Lake sediments that were exposed to anoxic and anoxic + algae conditions over an 8-week period. The anoxic + algae condition inhibited S reduction and enhanced the release of Mn but not the release of Fe (Figure 3). Langman et al. [21] indicated a substantial change in S oxidation states and the release of Mn into porewater during week 2 in the anoxic + algae condition that was not present during the anoxic condition (Figure 3). The anoxic and anoxic + algae conditions produced dissimilar trends in porewater Mn concentrations, similar trends in porewater Fe concentrations in the upper sediments, and similar trends of Fe and Mn porewater concentrations in the lower sediments (Figure 3). The Fe released into porewater in the upper sediments was primarily Fe<sup>2+</sup>, which ranged from 75% to 100% of the Fe detected in the porewater [21]. The anoxic + algae condition produced the greatest difference (+12,000 µg/L) in porewater Mn concentrations in the upper sediments during week 2, although both conditions produced similar porewater Mn concentrations by the end of the experiment. The goal of this investigation was to examine the sediments of

Langman et al. [21] for changes in Fe and Mn oxidation states and bonding environments over the course of the 8-week experiment, which may help explain the enhanced Mn mobility with the addition of the algal detritus that did not alter the mobility of Fe.

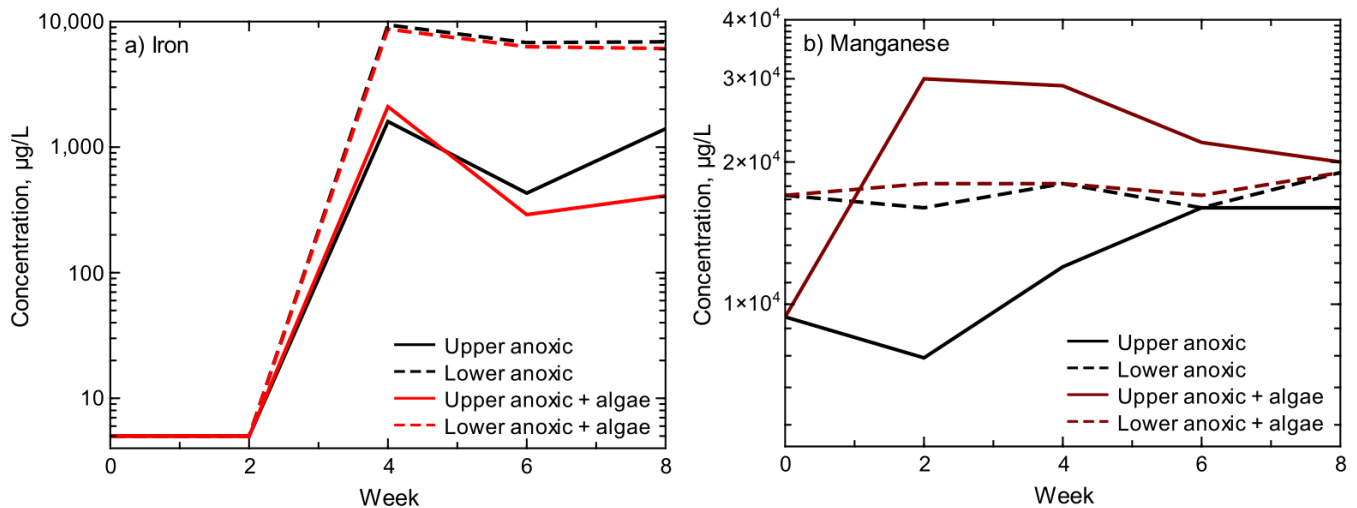


**Figure 3.** Iron and manganese concentrations in porewater extracted from sediment cores collected from Coeur d’Alene Lake that were exposed to anoxic and anoxic + algae conditions over an 8-week period (modified from [21]). The upper (2.5-cm depth) and lower (12.5-cm depth) iron and manganese concentrations are from the analysis of the porewater extracted from the corresponding sediment samples collected for X-ray absorption spectroscopy.

### 1.3. Lake Environment and Iron and Manganese Cycling

A substantial concentration of Mn along with the large presence of Fe in these lacustrine sediments allows these metals to participate in a variety of intertwined biogeochemical processes [52,53], such as degradation of humic acid [54,55], trace element cycling [56,57], and the coupled processes of carbon oxidation and anaerobic respiration [58]. The transformation of Fe and Mn in an anoxic sediment environment occurs through abiotic and microbially-catalyzed (e.g., bacteria, fungi, cyanobacteria, algal phototrophs) reactions, which can lead to the formation of Fe/Mn minerals and organometallic compounds that may or may not be soluble [59–67]. Reductive activation of dioxygen [O<sub>2</sub>] and production of superoxides/peroxides through metalloenzymes is a common degradation process of detrital organic matter where available Fe and Mn can play significant roles because of their bioavailability, multiple oxidation states, and coordination complexes [68–70]. Such enzymatic activity and metal-complex formation can create variable bonding environments with changes in Fe and Mn forms [68,69,71]. The role of Fe and Mn in such processes can be intertwined (e.g., Fe oxidation by Mn oxides [72]) and can produce differences in oxidation states, complexation (bonding environment), and solubility/mobility [73–75], which can be primary influences on the release and transport of metals from sediments into porewater and overlying waters [76–78]. The purpose of this examination of sediment Fe and Mn oxidation states and bonding environments was to evaluate potential indicators of a biogeochemical process that would enhance Mn mobility but not Fe mobility.

## 2. Study Area, Materials, and Methods

The Coeur d’Alene River Basin is located in the Coeur d’Alene Mountains of the Bitterroot Range. The quartzite and argillite containing the ore in the Coeur d’Alene Mining District have been mined since the 1880s and are part of the Mesoproterozoic Belt Supergroup composing the Coeur d’Alene Mountains [79]. The ore primarily consists of argentiferous galena [PbS] and sphalerite [(Zn,Fe)S] with associated carbonate zones consisting primarily of siderite [FeCO<sub>3</sub>] and ankerite [Ca(Fe,Mg,Mn)(CO<sub>3</sub>)<sub>2</sub>] [3,44,45]. An estimated 56 Mt of processed tailings with 900,000 t of Pb and 700,000 t of Zn have been

released into the basin floodplain along with unknown amounts of As, Cd, Cu, Fe, Hg, Mn, and Sb [80]. In addition to the processed tailings, waste rock containing an unknown amount of metal(loid)s was dumped in creek channels/floodplains as a legacy practice of waste disposal. The discarded tailings and waste rock were, and still are, being transported downstream by high streamflows, which distributed them throughout the river floodplain and into Coeur d'Alene Lake [3,35,45,81]. The lake continues to see fluctuations of metal concentrations in the water column, partially from the continued loading of metals from the Coeur d'Alene River [81] and partially from the release of metals from lake sediments during seasonal shifts in environmental conditions [29]. Currently, the lake does not experience substantive algal blooms, but lakebed sediments do contain organic matter concentrations of approximately 3–5% [21].

### 2.1. Study Design

This investigation is part of a series of analyses derived from laboratory experiments designed for examination of the potential release of metal(loid)s under current (anoxic) and possible future (anoxic + additional algal detritus (anoxic + algae)) seasonal conditions. The overall study was designed to replicate SWI conditions during the seasonal shift to anoxic conditions (control group), as well as a hypothetical condition of anoxia + algae (treatment group) to replicate possible future conditions that may include substantive algal blooms and the addition of greater organic matter (algal detritus) to the lakebed. In November 2017, sediment cores were collected from Aberdeen Lodge Bay (Figure 1, depth  $\approx$  15 m) in Coeur d'Alene Lake opposite the confluence of the Coeur d'Alene River. This sampling period was selected because the fall period represents the time of turnover and reoxygenation of the water column and upper sediments (outside of the perceived seasonal hypoxic/anoxic period that forms during summer).

### 2.2. Sediment Core Collection

As described by Langman et al. [21], sediment cores were collected in disinfected (70% EtOH, 30% ultrapure water) polyvinyl chloride core barrels (5.2-cm ID  $\times$  61-cm L) that were kept for 48 hr in a positive N<sub>2</sub> atmosphere prior to sampling. Using a Kajak–Brinkhurst gravity corer, the core barrels were allowed to free fall from 1 m below the lake surface for collection of sediment samples of 45–50 cm in depth (Figure 4). Head water in the core barrel was siphoned from each sample to minimize disturbance of the sediments during transport. After siphoning, cores were capped, flushed with N<sub>2</sub>, and stored upright in an N<sub>2</sub> atmosphere in gas-tight containers (Figure 4) for transport to the University of Idaho Lake Social Ecological Systems (LaSES) Laboratory in Coeur d'Alene, Idaho. At the time of the core collection, lake water was collected 1 m above the SWI using a disinfected, 2-L, Van Dorn sampler. Upon arrival at the LaSES Laboratory, core containers were checked for positive pressure and stored in the dark at 4.5 °C under an N<sub>2</sub> atmosphere.

### 2.3. Algae Collection and Column Loading

Algae was collected from Fernan Lake (Figure 1), a nearby eutrophic lake, by pumping water through an 80- $\mu$ m mesh net followed by centrifugation (3750 RCF for 15 min), solidification at  $-20$  °C, lyophilization for 24 h (Labconco FreeZone freeze dryer), and homogenization by the roll method [82–84]. To simulate the addition of algal detritus to the lakebed, 0.25 g of the homogenized algae were added to half of the cores along with 325 mL of Coeur d'Alene Lake water to all cores (half of the cores were in the control group and the other half in the treatment group). The amount of algal detritus added to the cores (118 g/m<sup>2</sup>) was based on previous sediment analyses of mesotrophic and eutrophic lakes in the Pacific Northwest, USA [48,85]. After input of the lake water or algae + lake water, the cores were capped, flushed with N<sub>2</sub>, and stored upright in the dark at 4.5 °C under an N<sub>2</sub> atmosphere for the 8-week experimental period [21].



**Figure 4.** Kajak–Brinkhurst gravity corer, free fall use from the University of Idaho Lake Social Ecological Systems boat in Coeur d’Alene Lake, and storage of the cores in the gas-tight containers with an N<sub>2</sub> source for atmosphere flushing.

#### 2.4. Column Experiment

Cores collected for this experiment were kept in the same anaerobic conditions (N<sub>2</sub> atmosphere) from which one control (anoxia) core and one treatment (anoxia + algae) core were removed and deconstructed every two weeks. The cores were deconstructed for the collection of sediment samples from 1-cm thick layers (slices) centered at 2.5 cm and 12.5 cm below the SWI. These sediments were collected for X-ray absorption spectroscopy (XAS) to examine Fe and Mn oxidation state distributions and bonding environments. These cores were the same cores and samples examined as part of the evaluation of S oxidation states and bonding environments [21]. The sediment samples were dewatered through centrifugation (3750 RCF for 15 min), dehydrated (lyophilized under vacuum for 24 h), and stored at  $-80^{\circ}\text{C}$ . The extracted porewater from centrifugation was analyzed for pH (calibrated to pH of 4 and 7) and oxidation-reduction potential or ORP (calibrated to a + 200 mV vs. Ag/AgCl standard). The 2.5-cm sample location represents the near SWI environment where redox-sensitive elements have concentrated [39], and the 12.5-cm sample location represents a possible restricted zone because of the low permeability in these silt/clay-dominated sediments. This deeper zone was selected for analysis to compare depth penetration of environmental changes that could influence Fe and Mn oxidation states and bonding environments. Deeper sample locations were not considered because of the presence of a volcanic ash layer (Mount St. Helens in 1980, Figure 2) about 15 cm below the SWI that restricts permeability and acts as a metal-sorbing substrate [86,87].

#### 2.5. X-ray Absorption Spectroscopy

The goal of this study was the temporal evaluation of shifts in sediment Fe and Mn oxidation states and bonding environments with the onset of anoxic conditions, as well as the addition of algal detritus at the SWI. Synchrotron-based XAS was used to discriminate Fe and Mn oxidation states and bonding environments for the sediment samples collected at 2.5 cm (upper) and 12.5 cm (lower) depths. Synchrotron-based XAS of the upper and lower sediment samples was performed at the Canadian Light Source’s 06B1-1 beamline (SXRMB) in Saskatchewan, Canada. A Si(111) monochromator at 06B1-1 can produce an incident beam energy of 1.7–10 keV. For this study, a  $3 \times 2$  mm bulk beam was used to collect fluorescence mode spectra for X-ray absorption near edge structure (XANES) and extended

X-ray absorption fine structure (EXAFS) analysis. The spectra were processed with the XAS program ATHENA [88]. K-edge energies for the reference materials were determined as the maxima of the first derivative and were shifted to the theoretical values to account for beamline flux. Each environmental sample was scanned twice to determine if additional scans were needed to reduce the signal-to-noise ratio. Random duplicate samples were scanned for comparison of spectra response to the primary sample. The environmental spectra were calibrated to the energy shift apparent from the applicable reference material, and the spectrum was edge-step normalized (maximum 15–80 eV normalization range).

An element's oxidation state distribution can be interpreted from the XANES region of the spectra [89,90]. Oxidation state distributions of Fe and Mn were determined with ATHENA's linear combination fitting (LCF) capability [88] within a K-edge range of  $-20$  eV to  $+30$  eV. The goal of the LCF analysis was to discriminate the oxidation state distributions of Fe and Mn by fitting spectra from common Fe and Mn oxidation states in reference materials. LCF was used to reconstruct each sample spectrum using reference material spectra of pyrite [ $\text{Fe}^{2+}\text{S}_2$ ] and goethite [ $\text{Fe}^{3+}\text{O}(\text{OH})$ ] for Fe and rhodochrosite [ $\text{Mn}^{2+}\text{CO}_3$ ], Mn(III) oxide [ $\text{Mn}^{3+}_2\text{O}_3$ ], and ramsdellite [ $\text{Mn}^{4+}\text{O}_2$ ] for Mn.

An element's coordination number, bond length, and/or local disorder of adjacent atoms can be evaluated through interpretation of the EXAFS region [91], which is a reflection of ejected photoelectrons interacting with the electrons of surrounding atoms (scatterers) or what is described as the bonding environment [89,92,93]. The EXAFS region of the sample spectra was analyzed for relative shifts in adjacent atom characteristics (e.g., bond length) through changes in 1st and 2nd sphere spectra in frequency filtered (Fourier transformation with  $k$ -weight = 2 and Hanning window (or cosine-squared taper))  $R$  space—magnitude ( $\chi(R)$ ) and real number ( $\text{Re}[\chi(R)]$ ) portions. The resulting complex number of the transformed spectra (Fourier transformed  $\chi(R)$  in Å) has real and imaginary numbers that complete the complex number, which is a reflection of the magnitude of the shell and bonding environment response (e.g., scatterer number and disorder) to the electron wavefunction [90,94,95]. Well-differentiated peaks in  $\chi(R)$  can indicate primary shells in the bonding environment, although the alteration of  $\chi(k)$  to  $\chi(R)$  shifts interpreted bond lengths approximately  $0.2$ – $0.5$  Å [90].

Given the substantial number of possible Fe and Mn bonds, more than one type of neighboring atom in each environmental sample (EXAFS spectra is a composite response of all bonds), and shifts in interpreted bond lengths with spectra transformation, the changes in lake sediment Fe and Mn bonding environments were viewed as relative differences between conditions and with time (temporal shifts with progression of the experiment). Shifts in the bonding environment reflect changes in magnitude responses and relative radial distances [96], such as differences in typical Fe bond lengths— $1.8$  Å for Fe–C [97–99],  $2.1$  Å for Fe–O [100],  $2.3$  Å for Fe–S [101], and  $2.5$  to  $3.1$  Å for Fe–Fe [90,102]. Mn–O bonds can be relatively inflexible, with bond lengths between  $1.7$  and  $2.2$  Å [103,104]. Mn–O bonds are shorter compared to Mn–C bonds, although Mn–O bonds will lengthen with lower Mn oxidation states [103,104]. With bond relocation of a portion of the Mn because of temporal changes in the environmental conditions, the composite response of the spectra will shift towards that increased bond type/length (e.g., radial distance change). Only the upper sediment samples were examined for bond environment shifts because of limited changes in the lower sediment oxidation state distributions.

### 3. Results

#### 3.1. Iron and Manganese Oxidation State Distribution

Examination of upper and lower sediment Fe oxidation states (Figure 5) indicated limited change in Fe oxidation state distribution (dominance of  $\text{Fe}^{3+}$ ) under anoxic and anoxic + algae conditions. Both the anoxic and anoxic + algae conditions produced favorable environments for oxidized Fe, with minor amounts of  $\text{Fe}^{2+}$  (3% to 40%) in weeks 2, 4, 6, or 8 for all conditions, except the anoxic upper sediments (Figure 5). Results from week 2 indicated the presence of  $\text{Fe}^{2+}$  in the deeper sediments under both conditions and under

the anoxic + algae condition in the upper sediments. The substantial release of Mn into porewater during week 2 in the upper sediments under the anoxic + algae condition (Figure 3) corresponds to the only detectable presence of  $\text{Fe}^{2+}$  in the upper sediments (Figure 5). Upper sediment porewater was neutral (pH range of 6.9 to 7.4) under both conditions throughout the experiment, and ORP varied (range of  $-83$  to  $180$  mV) but trended from oxidizing to reducing over the 8-week period. The greater presence of detectable  $\text{Fe}^{2+}$  in the deeper sediments under both conditions occurred under neutral (pH range of 6.7 to 7.4) and reducing (ORP range from  $-103$  to  $-30$  mV) conditions that did not have a substantial effect on the release of Mn into the porewater of these lower sediments (Figure 3).

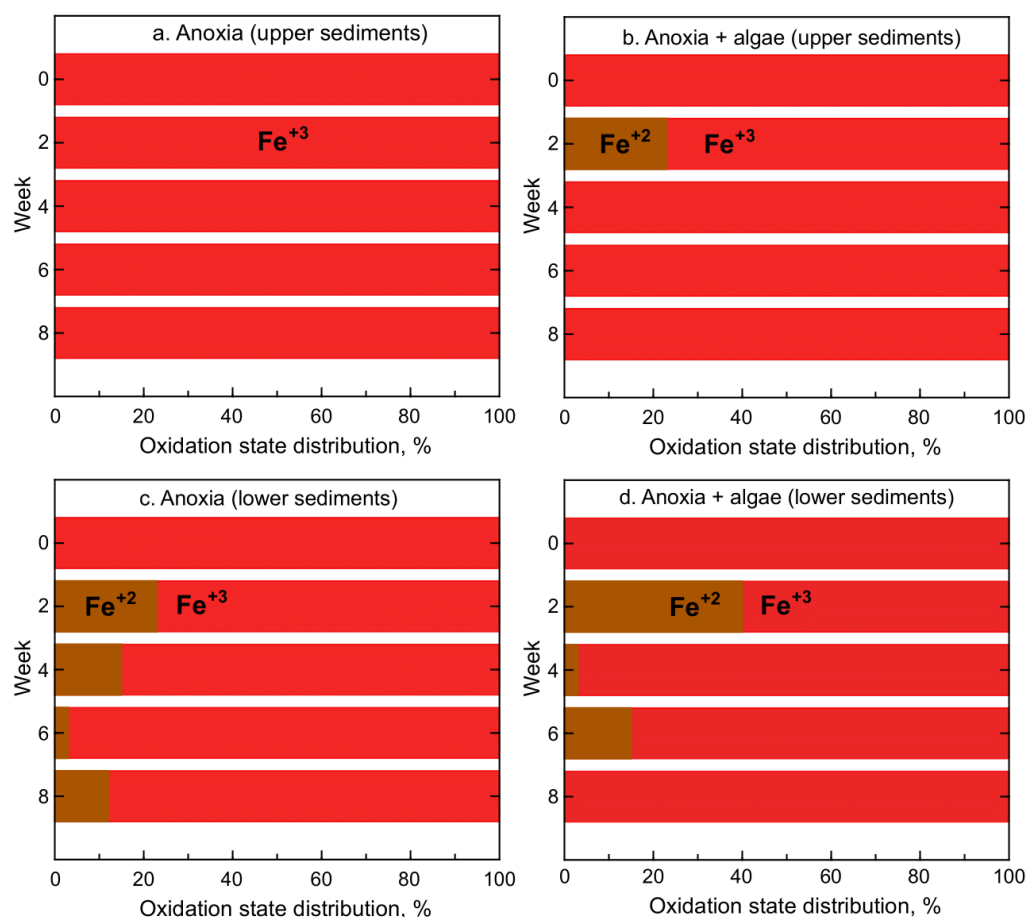


**Figure 5.** Distribution of iron oxidation states in upper and lower sediment samples of the control (anoxia) and treatment (anoxia + algae) cores over the course of the 8-week experiment.

The oxidation state distributions of Mn in the lower sediments indicated relatively similar patterns of  $\text{Mn}^{2+/3+}$  under the two conditions, except for the presence of a small amount of  $\text{Mn}^{4+}$  (2%) during week 2 in the anoxic + algae condition (Figure 6). The influence of anoxic and anoxic + algae conditions had a limited effect on Mn oxidation state distributions in the deeper sediments but did produce greater  $\text{Mn}^{3+}$  oxidation states (Figure 6) compared to the initial condition (week 0). This contrasts with the greater presence of reduced Fe in the lower sediments compared to the initial condition (Figure 5). The upper sediments indicated the greater presence of  $\text{Mn}^{3+}$ , particularly with the addition of algae, which had a strong influence on Mn oxidation states when compared to the anoxic condition (Figure 6). With the addition of algae, oxidation of Mn in the upper sediments progressed during the experiment and produced greater  $\text{Mn}^{3+}$ , as well as the presence of  $\text{Mn}^{4+}$  that was not identified with the anoxic condition (Figure 6). The presence of  $\text{Mn}^{4+}$  in the upper sediments under the anoxia + algae condition was not consistent with

progression of the experiment (not detected in week 6), yet results from week 8 indicated the least amount  $\text{Mn}^{2+}$  and greatest amount of  $\text{Mn}^{4+}$  under the anoxia + algae condition.

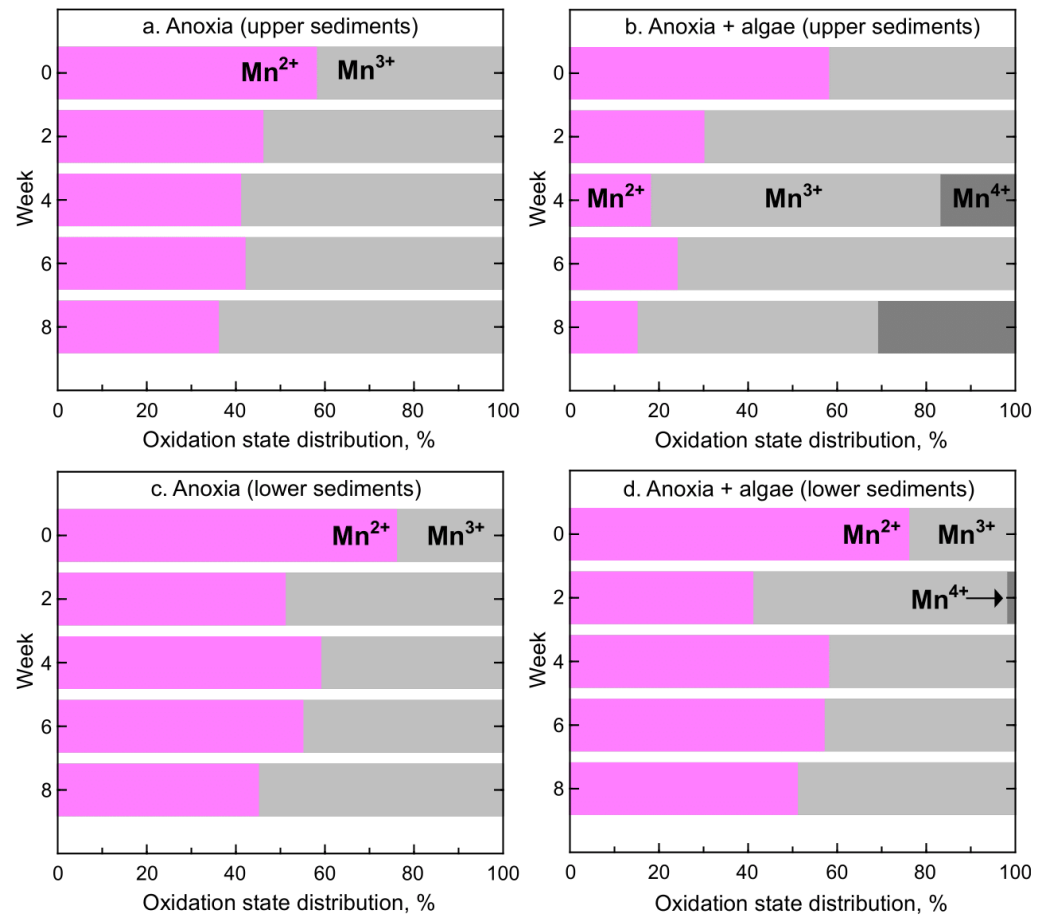


**Figure 6.** Distribution of manganese oxidation states in upper and lower sediment samples of the control (anoxia) and treatment (anoxia + algae) cores over the course of the 8-week experiment.

### 3.2. Upper Sediment Iron and Manganese Bonding Environments

The Fe EXAFS spectra for the upper sediment anoxic condition did not indicate substantial bond shifts during the experiment, except for a small initial change from the pre-experiment condition and an additional shift in week 2 under the anoxic + algae condition (Figure 7). The small shortening of the composite bond lengths from the initial condition suggests slightly more Fe–O and/or Fe–C bonds, which are shorter than Fe–Fe and Fe–S bonds [90,97–102]. With the start of the experiment and persistent anoxic conditions, Fe bonds stabilized at shorter bond lengths (e.g., Fe–O and/or Fe–C bonds) and remained similar throughout the experiment under the anoxic and anoxic + algae conditions (Figure 7). The week 2 anoxic + algae shift consisted of an earlier 1st sphere magnitude response ( $\chi(R)$ ) that likely represents a greater mixed state system with an additional shift to shorter bond lengths (Figure 7b). This shift in Fe bonds is reflected in the shorter period in the oscillation of the week 2 real portion ( $\text{Re}[\chi(R)]$ ) of the transformed spectra (Figure 7d) indicative of differences in near-neighbor coordination shells [90]. This slight shift in the Fe bonding environment during week 2 of the anoxic + algae condition corresponds to the increase in  $\text{Fe}^{2+}$  (Figure 5) and the greater release of Mn into porewater (Figure 3). The apparent change in the sediment/porewater environment resulted in redox changes that produced a shift towards shorter Fe bond lengths with multiple scattering paths (broader, lower magnitude peak) that dampened the backscatter response (EXAFS region is a sum of the backscattered waves [105]).

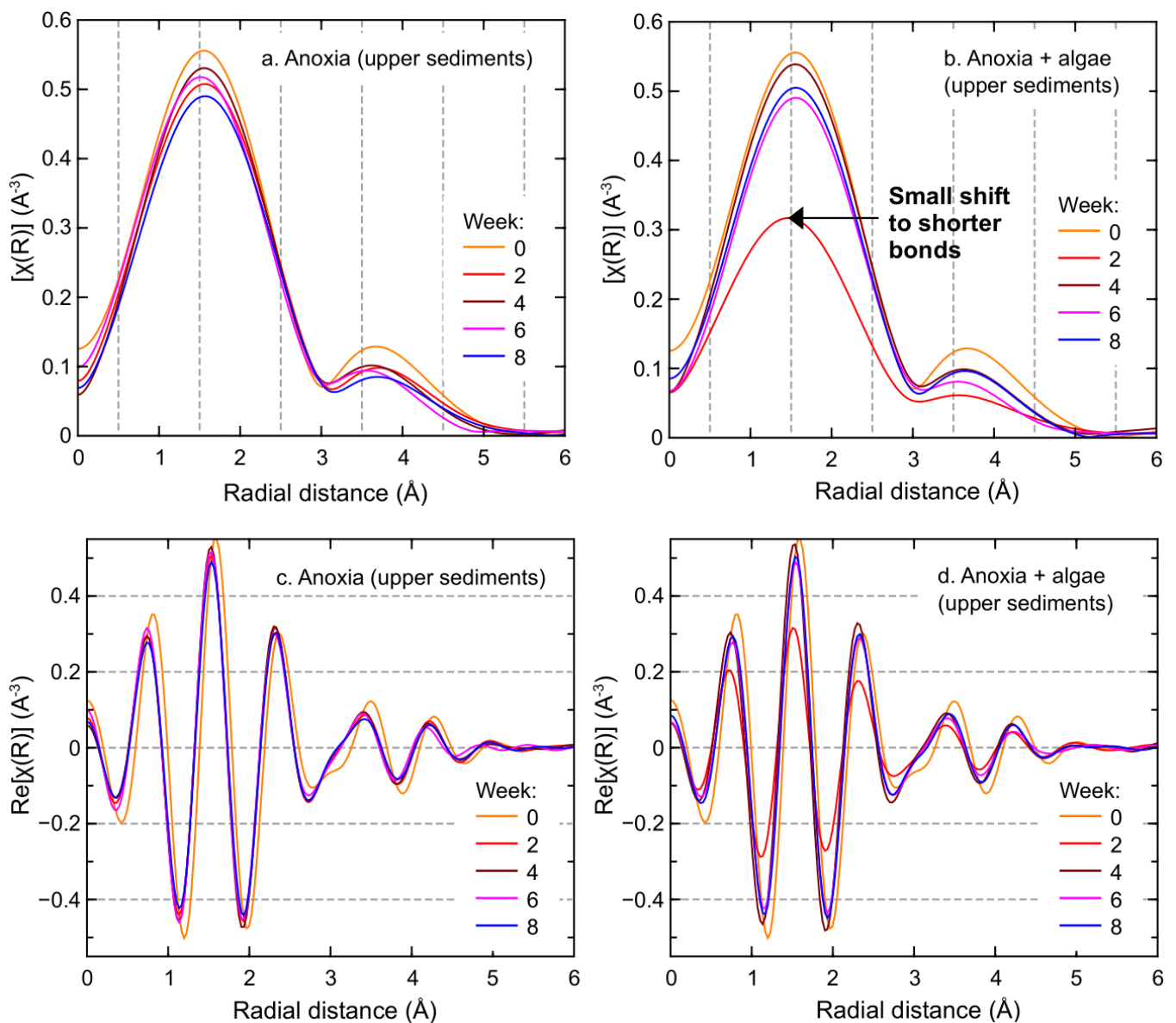


**Figure 7.** Fourier transformation of iron EXAFS spectra: magnitude ( $\chi(R)$ ) and real portion ( $\text{Re}[\chi(R)]$ ) for upper sediments of the control (anoxia) and treatment (anoxia + algae) cores over the course of the 8-week experiment.

The bonding environment for Mn under the anoxic condition indicated a trend towards longer bond lengths from the initial condition to week 8 (Figure 8). This small shift towards longer Mn bonds under anoxic conditions produced a week 8 dampening effect in the wave backscatter that reduced the period and amplitude of the oscillations (Figure 8c). With the addition of algae, the EXAFS spectra indicated substantial variation in the Mn bonding environment over the course of the experiment, such as the longer bond lengths during week 2 and the shorter bond lengths during weeks 4 and 6 (Figure 8b,d). Under this variable bonding environment, the backscatter oscillations indicated substantial shifts in period and amplitude (Figure 8d) that reflect the significant temporal shifts in Mn oxidation states (Figure 6). The shorter bond lengths in week 4 correspond to the detection of  $\text{Mn}^{4+}$  (Figure 6), which suggests shortened oxide bonds. The likely shifting of bond lengths and ligands (near-neighbor coordination spheres) suggests a cyclic process that fluxed with inputs from the degrading algae [68,70,72], which is highly visible in the real portion ( $\text{Re}[\chi(R)]$ ) of the transformed spectra for the anoxic + algae condition (Figure 8d).

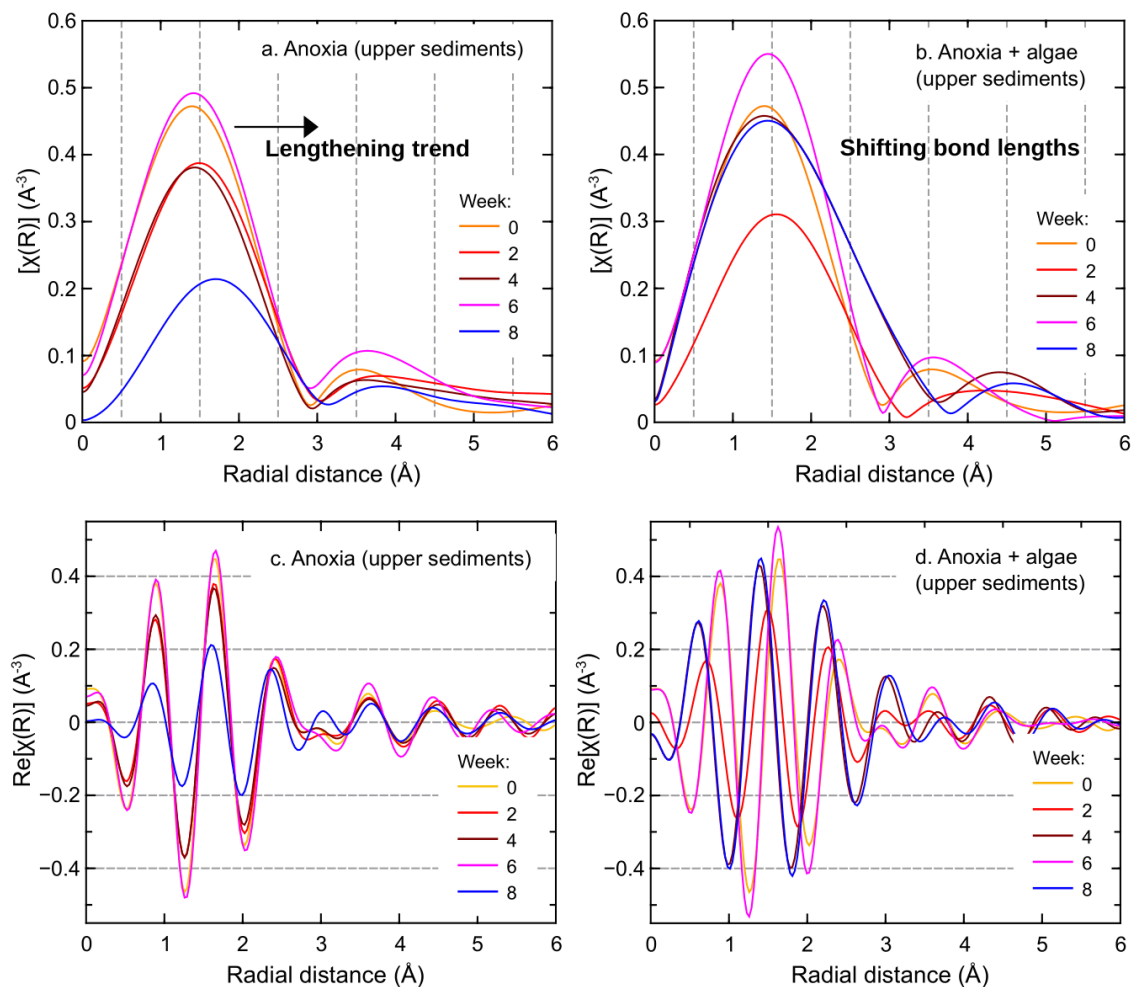


**Figure 8.** Fourier transformation of manganese EXAFS spectra: magnitude ( $\chi(R)$ ) and real portion ( $\text{Re}[\chi(R)]$ ) for upper sediments of the control (anoxia) and treatment (anoxia + algae) cores over the course of the 8-week experiment.

#### 4. Discussion

The results of this laboratory study may not reflect future in situ conditions, but the results are relevant if deposition of substantial organic matter occurs at select periods of future conditions in Coeur d'Alene Lake, such as increased algae deposition during the seasonal stratification. Fe and Mn have intertwined redox chemistries, and both metals have soluble reduced forms and generally insoluble (oxyhydr)oxides that will readily shift oxidation states with changes in redox conditions [20]. The difference in the  $\text{Mn}^{3+}/\text{Mn}^{2+}$  half reaction ( $E^\circ = +1.50$  V) and the  $\text{Fe}^{3+}/\text{Fe}^{2+}$  half reaction ( $E^\circ = +0.67$  V) can discriminate their roles in biogeochemical cycling because of the greater energy to be derived from Mn redox reactions, although redox potentials will vary with pH and temperature [106–108]. The anoxic + algae conditions were expected to provide additional carbon and nitrogen for the stimulation of microbial populations that could produce dissimilatory metal reduction with algae oxidation [109,110], which would correspond to the previous identification of primarily reduced S in the deeper sediments (both conditions), an increasing trend in reduced S under upper sediment anoxia, and variable S oxidation states with the addition of the algae [21]. Instead of acting as an electron acceptor, the microbial community appears to have assimilated or used sediment-bound Fe as an electron shuttle (e.g., extracellular electron transfer [111]) and likely formed organo-Mn complexes by enzymatic processes, where Mn can be relatively stable in the  $\text{Mn}^{3+}$  oxidation state (Figure 9) [112–114]. Given the general insolubility of  $\text{Fe}^{3+}$  (oxyhydr)oxides [115] and the

neutral pH of the porewater throughout the experiment, the Fe likely were sediment-bound oxides or were held in extracellular locations (cell outer surface or periplasm with Fe<sup>2+</sup> pump out) that avoid intracellular Fe precipitation and Fe<sup>2+</sup> toxicity [111,116,117]. These sediment-bound, extracellular locations may be why Fe<sup>3+</sup> was predominantly identified in the sediment samples (Figure 5) along with the release of primarily Fe<sup>2+</sup> to porewater. The Fe<sup>4+</sup> oxidation state of the example enzymatic process (Figure 9) was not analyzed in this experiment since Fe<sup>4+</sup> exists only temporarily as an electron shuttle, and the Fe is stabilized as Fe<sup>3+</sup> [118]. Given the presence of small concentrations of Fe<sup>3+</sup> in porewater (0% to 25%), some Fe<sup>3+</sup> chelates [119] may have formed and been released into the solution as part of such enzymatic processes.

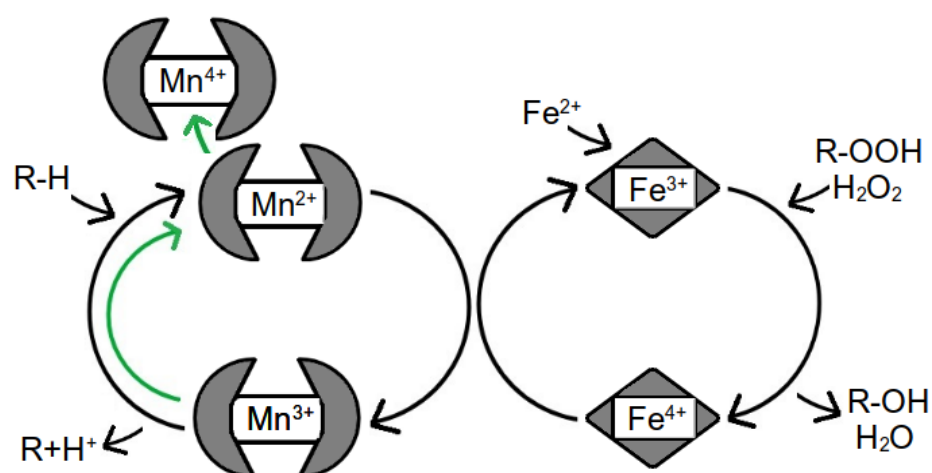


**Figure 9.** Schematic of possible enzymatic manganese cycling in the presence of detrital organic matter. The green arrow represents a potential pathway of an oxidase that forms Mn<sup>4+</sup> complexes (adapted from [112]).

Organo-complexed Mn can be formed by enzymatic activity where oxidized Fe is used as an electron shuttle to oxidize Mn<sup>2+</sup> to Mn<sup>3+,4+</sup> and produce Mn-oxalate/lactate chelates (Figure 9) [112,120]. Such processes keep Fe oxidized (Fe<sup>3+</sup>) while oxidizing Mn and producing various Mn chelates under anoxic conditions [121]. The strong prevalence of Mn<sup>3+</sup>, occasional presence of Mn<sup>4+</sup> (Figure 6), variation in the bonding environment of Mn in the anoxic + algae condition (Figure 8), and large release of Mn into porewater early in the experiment (Figure 3) indicate the early formation of water-soluble, multidentate Mn chelates (e.g., aminopolycarboxylic acids [122]) along with sediment-bound, enzyme-incorporated Mn<sup>3+,4+</sup> [123]. Oxidoreductase enzymes, such as Mn peroxidase, are present in almost all known bacteria and fungi [73], and they can provide the mechanism for algae degradation and Mn oxidation and mobility [113,120]. With microbially facilitated Mn<sup>2+</sup> oxidation, Mn<sup>3+/4+</sup> can be stabilized through bonding with carboxylic acids, which form compounds that can further oxidize degrading organic matter in an anoxic environment [66,112,120]. Such microbially facilitated activity likely produced the presence of primarily oxidized Fe in the sediments (Figure 5) and relatively stable Fe bonding environments under both conditions (Figure 7) because of the existing presence of available organic matter and microbial populations. The stability of Fe under anoxic and anoxic + algae conditions is in contrast with the increased oxidation of Mn (Figure 6) and the variable Mn bonding environment with the addition of algae (Figure 8). This greater variability in Mn oxidation states and bonding environments indicates enhanced enzymatic oxidation and stabilization of higher Mn oxidation states with the greater availability of organic matter [123,124]. Such an enhancement to Mn-involved enzymatic processes (Figure 9), even under anoxic conditions, likely is responsible for the increased Mn oxidation (Figure 6), limited change in Fe oxidation (Figure 5), variable Mn bond lengths (Figure 8), and release of greater amounts of Mn into porewater under the anoxic + algae conditions in the upper sediments (Figure 3).

With continued higher oxidation states of sediment Fe and Mn under the anoxic and anoxic + algae conditions, the mobility of Mn likely was enhanced by the formation of Mn chelates with greater enzymatic activity under the anoxic + algae condition, but the mobility of Fe was not influenced because it may have functioned as a sediment-bound electron shuttle. This scenario resulted in the similar release of Fe into porewater under both conditions in the lower and upper sediments (Figure 3). It is worthwhile to note that Fe mobility does increase with extended anoxic conditions (Figure 3), but the addition of algae to the SWI did not influence its mobility compared to the anoxic condition. With Fe mobility not influenced by the addition of the algae and the enhanced mobility of Mn likely because of the formation of Mn chelates, other metal(loid)s may not be substantially influenced by the increased presence of algal detritus at the SWI. Such results were noted by Langman et al. [21], where porewater As and Cd concentrations were similar under both conditions. With no additional increase in the release of Fe into porewater, there are no additional sorbing Fe surfaces in the solution that may enhance the transport of other metal(loid)s. Additionally, Mn chelates are not primary sorbing surfaces because of their relative stability or lower reactivity [125,126] compared to Mn oxides that are strong sorbing surfaces for other metal(loid)s [127–129]. However, the presence of additional organic matter and enhanced enzymatic activity could allow for the formation of other organometallic complexes that may be soluble and allow transport from the sediments.

## 5. Conclusions

Legacy mining practices allowed the hydrologic transport of tailings and waste rock from the Coeur d'Alene Mining District to Coeur d'Alene Lake, where an estimated 75 Mt of metal(loid)-contaminated sediments have entered the lake over the past 100+ years. Prior studies have indicated that the mining-contaminated sediments of Coeur d'Alene Lake undergo a seasonal anoxia period, which may evolve towards a seasonal period of anoxia plus additional algal detritus because of predicted algal blooms. The 8-week, benchtop experiments were conducted to simulate anoxic and anoxic + algae conditions for sediment cores collected from the lakebed. Examination of synchrotron X-ray absorption spectra for Fe and Mn in cored sediments indicated that anoxic conditions produced a relatively stable Fe oxidation state distribution and an increase in Mn oxidation over the experimental period. Correspondingly, the bonding environment of Fe did not significantly change over the course of the experiment, but the Mn bonding environment indicated substantial variation with the addition of the algae. This difference in oxidation state distribution and the bonding environment between Fe and Mn likely is a result of the incorporation of Fe as an electron shuttle in an enzymatic process that produces Mn<sup>3+/4+</sup> organo-complexes. This enzymatic process likely was enhanced with additional organic matter through introduction of the additional algae, which increased Mn oxidation and created a variable bonding environment. As part of this process, Fe is captured or retained at a higher oxidation state in the sediments under anoxic conditions, while Mn increases in oxidation and can be released as soluble Mn<sup>3+,4+</sup> chelates. This scenario likely explains the increase in porewater Mn concentrations with the addition of the algae. The lack of influence of algal detritus on sediment and porewater Fe, as well as the formation of soluble organo-Mn complexes, may limit the potential increase in the mobility of other metal(loid)s with the possible increase in deposition of algal detritus to the lakebed.

**Author Contributions:** Conceptualization, J.B.L., F.M.W. and J.G.M.; methodology, G.S., J.B.L., A.W.C., F.M.W. and J.G.M.; formal analysis, G.S. and J.B.L.; investigation, J.B.L., F.M.W. and J.G.M.; J.B.L., A.W.C., F.M.W. and J.G.M.; data curation, G.S. and J.B.L.; writing—original draft preparation, G.S. and J.B.L.; writing—review and editing, G.S., J.B.L., A.W.C., F.M.W. and J.G.M.; visualization, G.S. and J.B.L.; supervision, J.B.L.; project administration, J.B.L.; funding acquisition, J.B.L., F.M.W. and J.G.M. All authors have read and agreed to the published version of the manuscript.

**Funding:** This project was funded in part by the National Science Foundation Research Infrastructure Improvement award managed by Idaho EPSCoR under award number IIA-1301792 and the US Geological Survey 104b program as administered through the Idaho Water Resources Research Institute (grant #G16AP00050). Research described in this paper was performed at the Canadian Light Source (CLS), which is supported by the Canada Foundation for Innovation, Natural Sciences and Engineering Research Council of Canada, the University of Saskatchewan, the Government of Saskatchewan, Western Economic Diversification Canada, the National Research Council Canada, and the Canadian Institutes of Health Research.

**Data Availability Statement:** Spectra available upon request.

**Acknowledgments:** We wish to thank YongFeng Hu and Qunfeng Xiao of the Soft X-ray Microcharacterization Beamline at CLS for all their help and guidance.

**Conflicts of Interest:** The authors declare no conflict of interest. The funders had no role in the design of the study; in the collection, analyses, or interpretation of data; in the writing of the manuscript, or in the decision to publish the results.

## References

1. Harrington, J.M.; LaForce, M.J.; Rember, W.C.; Fendorf, S.E.; Rosenzweig, R.F. Phase Associations and Mobilization of Iron and Trace Elements in Coeur d'Alene Lake, Idaho. *Environ. Sci. Technol.* **1998**, *32*, 650–656. [[CrossRef](#)]
2. Horowitz, A.J.; Elrick, K.A.; Robbins, J.A.; Cook, R.B. A Summary of the Effects of Mining and Related Activities on the Sediment-Trace Element Geochemistry of Lake Coeur d'Alene, Idaho, USA. *J. Geochem. Explor.* **1995**, *52*, 135–144. [[CrossRef](#)]
3. National Research Council. *Superfund and Mining Megsites: Lessons from the Coeur d'Alene River Basin*; The National Academies of Sciences, Engineering, Medicine: Washington, DC, USA, 2005; p. 484.
4. Ciszewski, D.; Grygar, T.M. A Review of Flood-Related Storage and Remobilization of Heavy Metal Pollutants in River Systems. *Water. Air. Soil Pollut.* **2016**, *227*, 239. [[CrossRef](#)] [[PubMed](#)]
5. Gozzard, E.; Mayes, W.M.; Potter, H.A.B.; Jarvis, A.P. Seasonal and Spatial Variation of Diffuse (Non-Point) Source Zinc Pollution in a Historically Metal Mined River Catchment, UK. *Environ. Pollut.* **2011**, *159*, 3113–3122. [[CrossRef](#)]
6. Huettel, M.; Røy, H.; Precht, E.; Ehrenhauss, S. Hydrodynamical Impact on Biogeochemical Processes in Aquatic Sediments. In *The Interactions between Sediments and Water*; Kronvang, B., Ed.; Springer Netherlands: Dordrecht, The Netherlands, 2003; pp. 231–236.
7. Krantzberg, G. The Influence of Bioturbation on Physical, Chemical and Biological Parameters in Aquatic Environments: A Review. *Environ. Pollut. Ser. Ecol. Biol.* **1985**, *39*, 99–122. [[CrossRef](#)]
8. Schulz-Zunkel, C.; Krueger, F. Trace Metal Dynamics in Floodplain Soils of the River Elbe: A Review. *J. Environ. Qual.* **2009**, *38*, 1349–1362. [[CrossRef](#)]
9. Hamilton-Taylor, J.; Davison, W.; Morfett, K. The Biogeochemical Cycling of Zn, Cu, Fe, Mn, and Dissolved Organic C in a Seasonally Anoxic Lake. *Limnol. Oceanogr.* **1996**, *41*, 408–418. [[CrossRef](#)]
10. Morfett, K.; Davison, W.; Hamilton-Taylor, J. Trace Metal Dynamics in a Seasonally Anoxic Lake. *Environ. Geol. Water Sci.* **1988**, *11*, 107–114. [[CrossRef](#)]
11. Palmer, M.J.; Chételat, J.; Richardson, M.; Jamieson, H.E.; Galloway, J.M. Seasonal Variation of Arsenic and Antimony in Surface Waters of Small Subarctic Lakes Impacted by Legacy Mining Pollution near Yellowknife, NT, Canada. *Sci. Total Environ.* **2019**, *684*, 326–339. [[CrossRef](#)]
12. Gadd, G.M. Microbial Influence on Metal Mobility and Application for Bioremediation. *Geoderma* **2004**, *122*, 109–119. [[CrossRef](#)]
13. Langman, J.B.; Behrens, D.; Moberly, J.G. Seasonal Formation and Stability of Dissolved Metal Particles in Mining-Impacted, Lacustrine Sediments. *J. Contam. Hydrol.* **2020**, *232*, 103655. [[CrossRef](#)] [[PubMed](#)]
14. Martin, A.J.; Pedersen, T.F. Seasonal and Interannual Mobility of Arsenic in a Lake Impacted by Metal Mining. *Environ. Sci. Technol.* **2002**, *36*, 1516–1523. [[CrossRef](#)] [[PubMed](#)]
15. Ni, Z.; Wang, S.; Wang, Y. Characteristics of Bioavailable Organic Phosphorus in Sediment and Its Contribution to Lake Eutrophication in China. *Environ. Pollut.* **2016**, *219*, 537–544. [[CrossRef](#)] [[PubMed](#)]
16. Sarmiento, A.M.; Caraballo, M.A.; Sanchez-Rodas, D.; Nieto, J.M.; Parviainen, A. Dissolved and Particulate Metals and Arsenic Species Mobility along a Stream Affected by Acid Mine Drainage in the Iberian Pyrite Belt (SW Spain). *Appl. Geochem.* **2012**, *27*, 1944–1952. [[CrossRef](#)]
17. Smith, K.S.; Huyck, H.L.O. An Overview of the Abundance, Relative Mobility, Bioavailability, and Human Toxicity of Metals. In *The Environmental Geochemistry of Mineral Deposits: Part A: Processes, Techniques and Health Issues*; Plumlee, G.S., Logsdon, M.J., Filipek, L.F., Eds.; Society of Economic Geologists: Littleton, CO, USA, 1999; Volume 6A, pp. 29–70, ISBN 978-1-62949-013-7.
18. Wang, F.; Liu, C.; Liang, X.; Wei, Z. Remobilization of Trace Metals Induced by Microbiological Activities near Sediment-Water Interface, Aha Lake, Guiyang. *Chin. Sci. Bull.* **2003**, *48*, 2352–2356. [[CrossRef](#)]
19. Violante, A.; Cozzolino, V.; Perelomov, L.; Caporale, A.G.; Pigna, M. Mobility and Bioavailability of Heavy Metals and Metalloids in Soil Environments. *J. Soil Sci. Plant Nutr.* **2010**, *10*, 268–292. [[CrossRef](#)]

20. Davison, W. Iron and Manganese in Lakes. *Earth-Sci. Rev.* **1993**, *34*, 119–163. [[CrossRef](#)]
21. Langman, J.B.; Ali, J.D.; Child, A.W.; Wilhelm, F.M.; Moberly, J.G. Sulfur Species, Bonding Environment, and Metal Mobilization in Mining-Impacted Lake Sediments: Column Experiments Replicating Seasonal Anoxia and Deposition of Algal Detritus. *Minerals* **2020**, *10*, 849. [[CrossRef](#)]
22. Balistrieri, L.S.; Bookstrom, A.A.; Box, S.E.; Ikramuddin, M. *Drainage from Adits and Tailings Piles in the Coeur d'Alene Mining District, Idaho: Sampling, Analytical Methods and Results*; US Geological Survey Open-File Report; U.S. Geological Survey: Reston, VA, USA, 1998; p. 19.
23. Horowitz, A.J.; Elrick, K.A.; Robbins, J.A.; Cook, R.B. Effect of Mining and Related Activities on the Sediment Trace Element Geochemistry of Lake Coeur d'Alene, Idaho, USA Part II: Subsurface Sediments. *Hydrol. Process.* **1995**, *9*, 35–54. [[CrossRef](#)]
24. Paulson, A.J. Biogeochemical Removal of Zn and Cd in the Coeur d'Alene River (Idaho, USA), Downstream of a Mining District. *Sci. Total Environ.* **2001**, *278*, 31–44. [[CrossRef](#)]
25. Balistrieri, L.S.; Box, S.E.; Bookstrom, A.A.; Hooper, R.L.; Mahoney, J.B. *Impacts of Historical Mining in the Coeur d'Alene River Basin*; Bulletin; U.S. Geological Survey: Reston, VA, USA, 2010.
26. Woods, P.F. *Role of Limnological Processes in Fate and Transport of Nitrogen and Phosphorous Loads Delivered into Coeur d'Alene Lake and Lake Pend Oreille, Idaho, and Flathead Lake, Montana*; U.S. Geological Survey: Reston, VA, USA, 2004; p. 44.
27. La Force, M.J.; Hansel, C.M.; Fendorf, S. Arsenic Speciation, Seasonal Transformations, and Co-Distribution with Iron in a Mine Waste-Influenced Palustrine Emergent Wetland. *Environ. Sci. Technol.* **2000**, *34*, 3937–3943. [[CrossRef](#)]
28. U.S. Environmental Protection Agency. *Optimization Review Report: Remedial Process Optimization Study: Lake Coeur d'Alene, Bunker Hill Mining and Metallurgical Site, Operable Unit 03, Coeur d'Alene, Kootenai County, Idaho*; U.S. Environmental Protection Agency: Coeur d'Alene, ID, USA, 2020; p. 76.
29. Wood, M.S.; Beckwith, M.A. *Coeur d'Alene Lake, Idaho: Insights Gained from Limnological Studies of 1991–92 and 2004–06*; U.S. Geological Survey: Reston, VA, USA, 2008; p. 40.
30. Arora, B.; Şengör, S.S.; Spycher, N.F.; Steefel, C.I. A Reactive Transport Benchmark on Heavy Metal Cycling in Lake Sediments. *Comput. Geosci.* **2015**, *19*, 613–633. [[CrossRef](#)]
31. Cummings, D.E.; March, A.W.; Bostick, B.; Spring, S.; Caccavo, F.; Fendorf, S.; Rosenzweig, R.F. Evidence for Microbial Fe(III) Reduction in Anoxic, Mining-Impacted Lake Sediments (Lake Coeur d'Alene, Idaho). *Appl. Environ. Microbiol.* **2000**, *66*, 154–162. [[CrossRef](#)]
32. Aiken, G.R.; Hsu-Kim, H.; Ryan, J.N. Influence of Dissolved Organic Matter on the Environmental Fate of Metals, Nanoparticles, and Colloids. *Environ. Sci. Technol.* **2011**, *45*, 3196–3201. [[CrossRef](#)]
33. Haus, K.L.; Hooper, R.L.; Strumness, L.A.; Mahoney, J.B. Analysis of Arsenic Speciation in Mine Contaminated Lacustrine Sediment Using Selective Sequential Extraction, HR-ICPMS and TEM. *Appl. Geochem.* **2008**, *23*, 692–704. [[CrossRef](#)]
34. Kretzschmar, R.; Schäfer, T. Metal Retention and Transport on Colloidal Particles in the Environment. *Elements* **2005**, *1*, 205–210. [[CrossRef](#)]
35. Langman, J.B.; Torso, K.; Moberly, J.G. Seasonal and Basinal Influences on the Formation and Transport of Dissolved Trace Metal Forms in a Mining-Impacted Riverine Environment. *Hydrology* **2018**, *5*, 35. [[CrossRef](#)]
36. Plathe, K.L.; von der Kammer, F.; Hassellöv, M.; Moore, J.N.; Murayama, M.; Hofmann, T.; Hochella, M.F. The Role of Nanominerals and Mineral Nanoparticles in the Transport of Toxic Trace Metals: Field-Flow Fractionation and Analytical TEM Analyses after Nanoparticle Isolation and Density Separation. *Geochim. Cosmochim. Acta* **2013**, *102*, 213–225. [[CrossRef](#)]
37. Clark, G.M.; Mebane, C.A. *Sources, Transport and Trends for Selected Trace Metals and Nutrients in the Coeur d'Alene and Spokane River Basins, Northern Idaho, 1990–2013*; U.S. Geological Survey: Reston, VA, USA, 2014; p. 62.
38. Kuwabara, J.S.; Topping, B.R.; Woods, P.F.; Carter, J.L. Free Zinc Ion and Dissolved Orthophosphate Effects on Phytoplankton from Coeur d'Alene Lake, Idaho. *Environ. Sci. Technol.* **2007**, *41*, 2811–2817. [[CrossRef](#)]
39. Morra, M.J.; Carter, M.M.; Rember, W.C.; Kaste, J.M. Reconstructing the History of Mining and Remediation in the Coeur d'Alene, Idaho Mining District Using Lake Sediments. *Chemosphere* **2015**, *134*, 319–327. [[CrossRef](#)]
40. Woods, P.F.; Beckwith, M.A. *Nutrient and Trace-Element Enrichment of Coeur d'Alene Lake, Idaho*; U.S. Geological Survey: Reston, VA, USA, 1997; p. 93.
41. Harrington, J.M.; Fendorf, S.E.; Rosenzweig, R.F. Biotic Generation of Arsenic(III) in Metal(Loid)-Contaminated Freshwater Lake Sediments. *Environ. Sci. Technol.* **1998**, *32*, 2425–2430. [[CrossRef](#)]
42. Pedersen, T.F. A Comment on the Future Environmental Status of Coeur d'Alene Lake, Idaho. *Northwest Sci.* **1996**, *70*, 179–182.
43. Şengör, S.S.; Spycher, N.F.; Ginn, T.R.; Sani, R.K.; Peyton, B. Biogeochemical Reactive–Diffusive Transport of Heavy Metals in Lake Coeur d'Alene Sediments. *Appl. Geochem.* **2007**, *22*, 2569–2594. [[CrossRef](#)]
44. Balistrieri, L.S.; Box, S.E.; Tonkin, J.W. Modeling Precipitation and Sorption of Elements during Mixing of River Water and Porewater in the Coeur d'Alene River Basin. *Environ. Sci. Technol.* **2003**, *37*, 4694–4701. [[CrossRef](#)]
45. Balistrieri, L.S.; Blank, R.G. Dissolved and Labile Concentrations of Cd, Cu, Pb, and Zn in the South Fork Coeur d'Alene River, Idaho: Comparisons among Chemical Equilibrium Models and Implications for Biotic Ligand Models. *Appl. Geochem.* **2008**, *23*, 3355–3371. [[CrossRef](#)]
46. Gao, Y.; Kan, A.T.; Tomson, M.B. Critical Evaluation of Desorption Phenomena of Heavy Metals from Natural Sediments. *Environ. Sci. Technol.* **2003**, *37*, 5566–5573. [[CrossRef](#)]

47. Hoffmann, S.R.; Shafer, M.M.; Armstrong, D.E. Strong Colloidal and Dissolved Organic Ligands Binding Copper and Zinc in Rivers. *Environ. Sci. Technol.* **2007**, *41*, 6996–7002. [[CrossRef](#)]
48. Child, A.W.; Moore, B.C.; Vervoort, J.D.; Beutel, M.W. Bioavailability and Uptake of Smelter Emissions in Freshwater Zooplankton in Northeastern Washington, USA Lakes Using Pb Isotope Analysis and Trace Metal Concentrations. *Environ. Pollut.* **2018**, *238*, 348–358. [[CrossRef](#)]
49. Farley, M. Eutrophication in Fresh Waters: An International Review. In *Encyclopedia of Lakes and Reservoirs*; Bengtsson, L., Herschy, R.W., Fairbridge, R.W., Eds.; Springer Netherlands: Dordrecht, The Netherlands, 2012; pp. 258–270, ISBN 978-1-4020-4410-6.
50. Toevs, G.; Morra, M.J.; Winowiecki, L.; Strawn, D.; Polizzotto, M.L.; Fendorf, S. Depositional Influences on Porewater Arsenic in Sediments of a Mining-Contaminated Freshwater Lake. *Environ. Sci. Technol.* **2008**, *42*, 6823–6829. [[CrossRef](#)]
51. Bostick, B.C.; Hansel, C.M.; Fendorf, S. Seasonal Fluctuations in Zinc Speciation within a Contaminated Wetland. *Environ. Sci. Technol.* **2001**, *35*, 3823–3829. [[CrossRef](#)]
52. Boyle, J. Redox Remobilization and the Heavy Metal Record in Lake Sediments: A Modelling Approach. *J. Paleolimnol.* **2001**, *26*, 423–431. [[CrossRef](#)]
53. Boudreau, B.P. Metals and Models: Diagenic Modelling in Freshwater Lacustrine Sediments. *J. Paleolimnol.* **1999**, *22*, 227–251. [[CrossRef](#)]
54. Stone, A.T.; Morgan, J.J. Reduction and Dissolution of Manganese(III) and Manganese(IV) Oxides by Organics. 1. Reaction with Hydroquinone. *Environ. Sci. Technol.* **1984**, *18*, 450–456. [[CrossRef](#)] [[PubMed](#)]
55. Sunda, W.G.; Kieber, D.J. Oxidation of Humic Substances by Manganese Oxides Yields Low-Molecular-Weight Organic Substrates. *Nature* **1994**, *367*, 62–64. [[CrossRef](#)]
56. Murray, K.J.; Tebo, B.M. Cr(III) Is Indirectly Oxidized by the Mn(II)-Oxidizing Bacterium *Bacillus* Sp. Strain SG-1. *Environ. Sci. Technol.* **2007**, *41*, 528–533. [[CrossRef](#)] [[PubMed](#)]
57. Nelson, Y.M.; Lion, L.W.; Ghiorse, W.C.; Shuler, M.L. Production of Biogenic Mn Oxides by *Leptothrix Discophora* SS-1 in a Chemically Defined Growth Medium and Evaluation of Their Pb Adsorption Characteristics. *Appl. Environ. Microbiol.* **1999**, *65*, 175–180. [[CrossRef](#)] [[PubMed](#)]
58. Nealson, K.H.; Saffarini, D. Iron and Manganese in Anaerobic Respiration: Environmental Significance, Physiology, and Regulation. *Annu. Rev. Microbiol.* **1994**, *48*, 311–343. [[CrossRef](#)]
59. Andeer, P.F.; Learman, D.R.; McIlvin, M.; Dunn, J.A.; Hansel, C.M. Extracellular Haem Peroxidases Mediate Mn(II) Oxidation in a Marine *Roseobacter* Bacterium via Superoxide Production. *Environ. Microbiol.* **2015**, *17*, 3925–3936. [[CrossRef](#)]
60. Bargar, J.R.; Tebo, B.M.; Bergmann, U.; Webb, S.M.; Glatzel, P.; Chiu, V.Q.; Villalobos, M. Biotic and Abiotic Products of Mn(II) Oxidation by Spores of the Marine *Bacillus* Sp. Strain SG-1. *Am. Mineral.* **2005**, *90*, 143–154. [[CrossRef](#)]
61. Brouwers, G.-J.; de Vrind, J.P.M.; Corstjens, P.L.A.M.; Cornelis, P.; Baysse, C.; de Vrind-de Jong, E.W. CumA, a Gene Encoding a Multicopper Oxidase is Involved in Mn<sup>2+</sup> Oxidation in *Pseudomonas Putida* GB-1. *Appl. Environ. Microbiol.* **1999**, *65*, 1762–1768. [[CrossRef](#)]
62. Butterfield, C.N.; Soldatova, A.V.; Lee, S.-W.; Spiro, T.G.; Tebo, B.M. Mn(II,III) Oxidation and MnO<sub>2</sub> Mineralization by an Expressed Bacterial Multicopper Oxidase. *Proc. Natl. Acad. Sci. USA* **2013**, *110*, 11731–11735. [[CrossRef](#)] [[PubMed](#)]
63. Melton, E.D.; Swanner, E.D.; Behrens, S.; Schmidt, C.; Kappler, A. The Interplay of Microbially Mediated and Abiotic Reactions in the Biogeochemical Fe Cycle. *Nat. Rev. Microbiol.* **2014**, *12*, 797–808. [[CrossRef](#)] [[PubMed](#)]
64. Qin, X.; Sun, X.; Huang, H.; Bai, Y.; Wang, Y.; Luo, H.; Yao, B.; Zhang, X.; Su, X. Oxidation of a Non-Phenolic Lignin Model Compound by Two *Irpex Lacteus* Manganese Peroxidases: Evidence for Implication of Carboxylate and Radicals. *Biotechnol. Biofuels* **2017**, *10*, 103. [[CrossRef](#)] [[PubMed](#)]
65. Villalobos, M.; Toner, B.; Bargar, J.; Sposito, G. Characterization of the Manganese Oxide Produced by *Pseudomonas Putida* Strain MnB1. *Geochim. Cosmochim. Acta* **2003**, *67*, 2649–2662. [[CrossRef](#)]
66. Wong, D.W.S. Structure and Action Mechanism of Ligninolytic Enzymes. *Appl. Biochem. Biotechnol.* **2009**, *157*, 174–209. [[CrossRef](#)] [[PubMed](#)]
67. Zeiner, C.A.; Purvine, S.O.; Zink, E.; Wu, S.; Paša-Tolić, L.; Chaput, D.L.; Santelli, C.M.; Hansel, C.M. Mechanisms of Manganese(II) Oxidation by Filamentous Ascomycete Fungi Vary with Species and Time as a Function of Secretome Composition. *Front. Microbiol.* **2021**, *12*, 610497. [[CrossRef](#)]
68. Guo, M.; Corona, T.; Ray, K.; Nam, W. Heme and Nonheme High-Valent Iron and Manganese Oxo Cores in Biological and Abiological Oxidation Reactions. *ACS Cent. Sci.* **2019**, *5*, 13–28. [[CrossRef](#)]
69. Olivo, G.; Cussó, O.; Borrell, M.; Costas, M. Oxidation of Alkane and Alkene Moieties with Biologically Inspired Nonheme Iron Catalysts and Hydrogen Peroxide: From Free Radicals to Stereoselective Transformations. *JBIC J. Biol. Inorg. Chem.* **2017**, *22*, 425–452. [[CrossRef](#)]
70. Sahu, S.; Goldberg, D.P. Activation of Dioxygen by Iron and Manganese Complexes: A Heme and Nonheme Perspective. *J. Am. Chem. Soc.* **2016**, *138*, 11410–11428. [[CrossRef](#)]
71. Du, J.; Miao, C.; Xia, C.; Lee, Y.-M.; Nam, W.; Sun, W. Mechanistic Insights into the Enantioselective Epoxidation of Olefins by Bioinspired Manganese Complexes: Role of Carboxylic Acid and Nature of Active Oxidant. *ACS Catal.* **2018**, *8*, 4528–4538. [[CrossRef](#)]

72. Bryce, C.; Blackwell, N.; Schmidt, C.; Otte, J.; Huang, Y.-M.; Kleindienst, S.; Tomaszewski, E.; Schad, M.; Warter, V.; Peng, C.; et al. Microbial Anaerobic Fe(II) Oxidation—Ecology, Mechanisms and Environmental Implications. *Environ. Microbiol.* **2018**, *20*, 3462–3483. [[CrossRef](#)] [[PubMed](#)]
73. Chowdhary, P.; Shukla, G.; Raj, G.; Ferreira, L.F.R.; Bharagava, R.N. Microbial Manganese Peroxidase: A Ligninolytic Enzyme and Its Ample Opportunities in Research. *SN Appl. Sci.* **2018**, *1*, 45. [[CrossRef](#)]
74. Engelmann, X.; Monte-Pérez, I.; Ray, K. Oxidation Reactions with Bioinspired Mononuclear Non-Heme Metal–Oxo Complexes. *Angew. Chem. Int. Ed.* **2016**, *55*, 7632–7649. [[CrossRef](#)] [[PubMed](#)]
75. Sawant, S.C.; Wu, X.; Cho, J.; Cho, K.-B.; Kim, S.H.; Seo, M.S.; Lee, Y.-M.; Kubo, M.; Ogura, T.; Shaik, S.; et al. Water as an Oxygen Source: Synthesis, Characterization, and Reactivity Studies of a Mononuclear Nonheme Manganese(IV) Oxo Complex. *Angew. Chem.* **2010**, *49*, 8190–8194. [[CrossRef](#)] [[PubMed](#)]
76. Kappler, A.; Bryce, C.; Mansor, M.; Lueder, U.; Byrne, J.M.; Swanner, E.D. An Evolving View on Biogeochemical Cycling of Iron. *Nat. Rev. Microbiol.* **2021**, *19*, 360–374. [[CrossRef](#)] [[PubMed](#)]
77. Singh, S.K.; Subramanian, V.; Gibbs, R.J. Hydrous Fe and Mn Oxides—Scavengers of Heavy Metals in the Aquatic Environment. *Crit. Rev. Environ. Control.* **1984**, *14*, 33–90. [[CrossRef](#)]
78. Wojtkowska, M. Migration and Forms of Metals in Bottom Sediments of Czerniakowskie Lake. *Bull. Environ. Contam. Toxicol.* **2013**, *90*, 165–169. [[CrossRef](#)]
79. Leach, D.L.; Landis, G.P.; Hofstra, A.H. Metamorphic Origin of the Coeur d’Alene Base- and Precious-Metal Veins in the Belt Basin, Idaho and Montana. *Geology* **1988**, *16*, 122–125. [[CrossRef](#)]
80. Long, K.R. *Production and Disposal of Mill Tailings in the Coeur d’Alene Mining Region, Shoshone County, Idaho: Preliminary Estimates*; Open-File Report; U.S. Geological Survey: Reston, VA, USA, 1998.
81. Hickey, P.J.; McDaniel, P.A.; Strawn, D.G. Characterization of Iron- and Manganese-Cemented Redoximorphic Aggregates in Wetland Soils Contaminated with Mine Wastes. *J. Environ. Qual.* **2008**, *37*, 2375–2385. [[CrossRef](#)]
82. Ingamells, C.O.; Pitard, F.F. *Applied Geochemical Analysis*; Chemical Analysis 88; Wiley: New York, NY, USA, 1986; ISBN 0-471-83279-0.
83. Johnson, W.M.; Maxwell, J.A. *Rock and Mineral Analysis*, 2nd ed.; Wiley & Sons: New York, NY, USA, 1981; ISBN 978-0-471-02743-0.
84. Schüler, V.C.O. Chemical Analysis and Sample Preparation. In *Modern Methods of Geochemical Analysis*; Wainerdi, R.E., Uken, E.A., Eds.; Monographs in Geoscience; Springer US: Boston, MA, USA, 1971; pp. 53–71, ISBN 978-1-4684-1830-9.
85. Welch, E.B. Should Nitrogen Be Reduced to Manage Eutrophication If It Is Growth Limiting? Evidence from Moses Lake. *Lake Reserv. Manag.* **2009**, *25*, 401–409. [[CrossRef](#)]
86. Heap, M.J.; Reuschlé, T.; Farquharson, J.I.; Baud, P. Permeability of Volcanic Rocks to Gas and Water. *J. Volcanol. Geotherm. Res.* **2018**, *354*, 29–38. [[CrossRef](#)]
87. Jensen, L.C.; Becerra, J.R.; Escudey, M. *Impact of Physical/Chemical Properties of Volcanic Ash-Derived Soils on Mechanisms Involved during Sorption of Ionisable and Non-Ionisable Herbicides*; IntechOpen: Rijeka, Croatia, 2018; ISBN 978-1-78984-819-9.
88. Ravel, B.; Newville, M. ATHENA, ARTEMIS, HEPHAESTUS: Data Analysis for X-ray Absorption Spectroscopy Using IFEFFIT. *J. Synchrotron Radiat.* **2005**, *12*, 537–541. [[CrossRef](#)] [[PubMed](#)]
89. Alp, E.E.; Mini, S.M.; Ramanathan, M. *X-ray Absorption Spectroscopy: EXAFS and XANES—A Versatile Tool to Study the Atomic and Electronic Structure of Materials*; Department of Energy, Argonne National Laboratory: Lemont, IL, USA, 1990; pp. 25–36.
90. Newville, M. Fundamentals of XAFS. *Rev. Mineral. Geochem.* **2014**, *78*, 33–74. [[CrossRef](#)]
91. Sham, T.K. Nanoparticles and Nanowires: Synchrotron Spectroscopy Studies. *Int. J. Nanotechnol.* **2008**, *5*, 1194–1246. [[CrossRef](#)]
92. Gaur, A.; Shrivastava, B.D. Speciation Using X-ray Absorption Fine Structure (XAFS). *Rev. J. Chem.* **2015**, *5*, 361–398. [[CrossRef](#)]
93. Penner-Hahn, J.E. *X-ray Absorption Spectroscopy*; eLS: Hong Kong, China, 2005. [[CrossRef](#)]
94. Koningsberger, D.C.; Mojet, B.L.; van Dorssen, G.E.; Ramaker, D.E. XAFS Spectroscopy: Fundamental Principles and Data Analysis. *Top. Catal.* **2000**, *10*, 143–155. [[CrossRef](#)]
95. Koningsberger, D.C.; Ramaker, D.E. Applications of X-ray Absorption Spectroscopy in Heterogeneous Catalysis: EXAFS, Atomic XAFS, and Delta XANES. In *Handbook of Heterogeneous Catalysis*; American Cancer Society: Atlanta, GA, USA, 2008; pp. 774–803, ISBN 978-3-527-61004-4.
96. van Bokhoven, J.A.; Ressler, T.; de Groot, F.M.F.; Knopp-Gericke, G. Extended X-ray Absorption Fine-Structure Spectroscopy. *ChemInform* **2005**, *36*. [[CrossRef](#)]
97. Braga, D.; Grepioni, F.; Orpen, A.G. Nickel Carbonyl [Ni(CO)<sub>4</sub>] and Iron Carbonyl [Fe(CO)<sub>5</sub>]: Molecular Structures in the Solid State. *Organometallics* **1993**, *12*, 1481–1483. [[CrossRef](#)]
98. Chen, W.T.; Hsu, C.W.; Lee, J.F.; Pao, C.W.; Hsu, I.J. Theoretical Analysis of Fe K-Edge XANES on Iron Pentacarbonyl. *ACS Omega* **2020**, *5*, 4991–5000. [[CrossRef](#)]
99. Hanson, A.W. The Crystal Structure of Iron Pentacarbonyl. *Acta Crystallogr.* **1962**, *15*, 930–933. [[CrossRef](#)]
100. Hicks, L.J.; Bridges, J.C.; Gurman, S.J. Ferric Saponite and Serpentine in the Nakhilite Martian Meteorites. *Geochim. Cosmochim. Acta* **2014**, *136*, 194–210. [[CrossRef](#)]
101. Sayers, D.E.; Stern, E.A.; Herriott, J.R. Measurement of Fe–S Bond Lengths in Rubredoxin Using Extended X-ray Absorption Fine Structure (EXAFS). *J. Chem. Phys.* **1976**, *64*, 427–428. [[CrossRef](#)]

102. Pauling, L. Metal-Metal Bond Lengths in Complexes of Transition Metals. *Proc. Natl. Acad. Sci. USA* **1976**, *73*, 4290–4293. [[CrossRef](#)] [[PubMed](#)]
103. Gilbert, B.; Frazer, B.H.; Belz, A.; Conrad, P.G.; Nealson, K.H.; Haskel, D.; Lang, J.C.; Srajer, G.; De Stasio, G. Multiple Scattering Calculations of Bonding and X-ray Absorption Spectroscopy of Manganese Oxides. *J. Phys. Chem. A* **2003**, *107*, 2839–2847. [[CrossRef](#)]
104. Leto, D.F.; Jackson, T.A. Mn K-Edge X-ray Absorption Studies of Oxo- and Hydroxo-Manganese(IV) Complexes: Experimental and Theoretical Insights into Pre-Edge Properties. *Inorg. Chem.* **2014**, *53*, 6179–6194. [[CrossRef](#)]
105. Mastelaro, V.R.; Zanotto, E.D. X-ray Absorption Fine Structure (XAFS) Studies of Oxide Glasses—A 45-Year Overview. *Materials* **2018**, *11*, 204. [[CrossRef](#)]
106. Luther, G.W. The Role of One- and Two-Electron Transfer Reactions in Forming Thermodynamically Unstable Intermediates as Barriers in Multi-Electron Redox Reactions. *Aquat. Geochem.* **2010**, *16*, 395–420. [[CrossRef](#)]
107. LaRowe, D.E.; Carlson, H.K.; Amend, J.P. The Energetic Potential for Undiscovered Manganese Metabolisms in Nature. *Front. Microbiol.* **2021**, *12*, 1347. [[CrossRef](#)]
108. Straub, K.L.; Benz, M.; Schink, B. Iron Metabolism in Anoxic Environments at near Neutral PH. *FEMS Microbiol. Ecol.* **2001**, *34*, 181–186. [[CrossRef](#)]
109. Bradley, A.S.; Leavitt, W.D.; Johnston, D.T. Revisiting the Dissimilatory Sulfate Reduction Pathway. *Geobiology* **2011**, *9*, 446–457. [[CrossRef](#)]
110. Plugge, C.; Zhang, W.; Scholten, J.; Stams, A. Metabolic Flexibility of Sulfate-Reducing Bacteria. *Front. Microbiol.* **2011**, *2*, 81. [[CrossRef](#)] [[PubMed](#)]
111. He, S.; Barco, R.A.; Emerson, D.; Roden, E.E. Comparative Genomic Analysis of Neutrophilic Iron(II) Oxidizer Genomes for Candidate Genes in Extracellular Electron Transfer. *Front. Microbiol.* **2017**, *8*, 1584. [[CrossRef](#)] [[PubMed](#)]
112. Hofrichter, M. Review: Lignin Conversion by Manganese Peroxidase (MnP). *Enzyme Microb. Technol.* **2002**, *30*, 454–466. [[CrossRef](#)]
113. Quintanar, L.; Stoj, C.; Taylor, A.B.; Hart, P.J.; Kosman, D.J.; Solomon, E.I. Shall We Dance? How a Multicopper Oxidase Chooses Its Electron Transfer Partner. *Acc. Chem. Res.* **2007**, *40*, 445–452. [[CrossRef](#)] [[PubMed](#)]
114. Wariishi, H.; Valli, K.; Gold, M.H. Manganese(II) Oxidation by Manganese Peroxidase from the Basidiomycete Phanerochaete Chrysosporium. Kinetic Mechanism and Role of Chelators. *J. Biol. Chem.* **1992**, *267*, 23688–23695. [[CrossRef](#)] [[PubMed](#)]
115. Baumgartner, J.; Faivre, D. Iron Solubility, Colloids and Their Impact on Iron (Oxyhydr)Oxide Formation from Solution. *Earth-Sci. Rev.* **2015**, *150*, 520–530. [[CrossRef](#)]
116. Bennett, B.D.; Gralnick, J.A. Mechanisms of Toxicity by and Resistance to Ferrous Iron in Anaerobic Systems. *Free Radic. Biol. Med.* **2019**, *140*, 167–171. [[CrossRef](#)]
117. Schädler, S.; Burkhardt, C.; Hegler, F.; Straub, K.; Miot, J.; Benzerara, K. Formation of Cell-Iron-Mineral Aggregates by Phototrophic and Nitratereducing Anaerobic Fe (II)-Oxidizing Bacteria. *Geomicrobiol. J.* **2009**, *26*, 93–103. [[CrossRef](#)]
118. Sundaramoorthy, M.; Kishi, K.; Gold, M.H.; Poulos, T.L. The Crystal Structure of Manganese Peroxidase from Phanerochaete Chrysosporium at 2.06-Å Resolution. *J. Biol. Chem.* **1994**, *269*, 32759–32767. [[CrossRef](#)] [[PubMed](#)]
119. Nevin, K.P.; Lovley, D.R. Mechanisms for Fe(III) Oxide Reduction in Sedimentary Environments. *Geomicrobiol. J.* **2002**, *19*, 141–159. [[CrossRef](#)]
120. Kumar, A.; Chandra, R. Ligninolytic Enzymes and Its Mechanisms for Degradation of Lignocellulosic Waste in Environment. *Heliyon* **2020**, *6*, e03170. [[CrossRef](#)] [[PubMed](#)]
121. Abdel-Hamid, A.M.; Solbiati, J.O.; Cann, I.K.O. Chapter One—Insights into Lignin Degradation and Its Potential Industrial Applications. In *Advances in Applied Microbiology*; Sariaslani, S., Gadd, G.M., Eds.; Academic Press: Cambridge, MA, USA, 2013; Volume 82, pp. 1–28.
122. Bucheli-Witschel, M.; Egli, T. Environmental Fate and Microbial Degradation of Aminopolycarboxylic Acids. *FEMS Microbiol. Rev.* **2001**, *25*, 69–106. [[CrossRef](#)] [[PubMed](#)]
123. Soldatova, A.V.; Romano, C.A.; Tao, L.; Stich, T.A.; Casey, W.H.; Britt, R.D.; Tebo, B.M.; Spiro, T.G. Mn(II) Oxidation by the Multicopper Oxidase Complex Mnx: A Coordinated Two-Stage Mn(II)/(III) and Mn(III)/(IV) Mechanism. *J. Am. Chem. Soc.* **2017**, *139*, 11381–11391. [[CrossRef](#)] [[PubMed](#)]
124. Liu, W.; Hao, J.; Elzinga, E.J.; Piotrowiak, P.; Nanda, V.; Yee, N.; Falkowski, P.G. Anoxic Photogeochemical Oxidation of Manganese Carbonate Yields Manganese Oxide. *Proc. Natl. Acad. Sci. USA* **2020**, *117*, 22698–22704. [[CrossRef](#)] [[PubMed](#)]
125. López-Rayó, S.; Lucena, S.; Lucena, J.J. Chemical Properties and Reactivity of Manganese Chelates and Complexes in Solution and Soils. *J. Plant Nutr. Soil Sci.* **2014**, *177*, 189–198. [[CrossRef](#)]
126. Norvell, W.A. Reactions of Metal Chelates in Soils and Nutrient Solutions. In *Micronutrients in Agriculture*; John Wiley & Sons, Ltd.: Hoboken, NJ, USA, 1991; pp. 187–227, ISBN 978-0-89118-878-0.
127. McKenzie, R. The Adsorption of Lead and Other Heavy Metals on Oxides of Manganese and Iron. *Soil Res.* **1980**, *18*, 61–73. [[CrossRef](#)]

128. Dang, D.H.; Lenoble, V.; Durrieu, G.; Omanović, D.; Mullet, J.-U.; Mounier, S.; Garnier, C. Seasonal Variations of Coastal Sedimentary Trace Metals Cycling: Insight on the Effect of Manganese and Iron (Oxy)Hydroxides, Sulphide and Organic Matter. *Mar. Pollut. Bull.* **2015**, *92*, 113–124. [[CrossRef](#)]
129. Zhang, G.; Liu, F.; Liu, H.; Qu, J.; Liu, R. Respective Role of Fe and Mn Oxide Contents for Arsenic Sorption in Iron and Manganese Binary Oxide: An X-ray Absorption Spectroscopy Investigation. *Environ. Sci. Technol.* **2014**, *48*, 10316–10322. [[CrossRef](#)]

**Disclaimer/Publisher’s Note:** The statements, opinions and data contained in all publications are solely those of the individual author(s) and contributor(s) and not of MDPI and/or the editor(s). MDPI and/or the editor(s) disclaim responsibility for any injury to people or property resulting from any ideas, methods, instructions or products referred to in the content.